

**A.Stulov**  
**HEREDITARY FEATURES OF PIANO HAMMER**

Centre for Nonlinear Studies, Institute of Cybernetics at Tallinn Technical University  
 Akadeemia 21, Tallinn, 12618 Estonia  
 Tel: (+372) 620 4164; Fax: (+372) 620 4151  
 E-mail: [stulov@ioc.ee](mailto:stulov@ioc.ee)

*Based upon the large number of experimental data obtained using a special piano hammer testing device, it has been shown, that all the present-day piano hammers have as a quality the hysteretic type of the force-compression characteristics. Two mathematical hysteretic models can describe the dynamical behavior of the piano hammer. The first four-parameter nonlinear hysteretic model of piano hammer describes the hammer felt as a nonlinear standard viscoelastic body. The second new three-parameter hysteretic model is a nonlinear analogue of the Voigt model. The both models are based on an assumption that the hammer felt made of wool is a microstructured material possessing history-dependent properties. The equivalence of these models is proved for all the realistic values of hammer velocity. It has been shown that both models describe the dynamic hysteretic behavior of hammer felt in good agreement with experimental data. The experimental tests of the hammer permit the determination of the values of the stiffness and hereditary parameters of the hammer felt. This gives the possibility to simulate the process of the interaction of a hysteretic hammer with a string. The calculated flexible string motion and the string vibration spectra excited by different piano hammers are presented.*

This work was supported by the Estonian Science Foundation under Grant No. 5566, and the author participation at the XVth Session of the Russian Acoustical Society was funded in part through the U.S. Embassy in Tallinn.

The sound of the grand piano depends mostly on the detailed motion of strings excited by the impact of the hammer. Thus the creation of good theoretical models of the hammer and the hammer-string interaction are important problems for determining the sound produced by a piano. In the first model the hammer was assumed absolutely rigid. Although this model is far from being realistic, it was used for more than sixty years because of its simplicity.

The modern hammers have a wood core covered with one or two layers of compressed wool felt, whose stiffness increases from heavy bass hammers to light treble hammers to produce a good tone. One of the most important features of the hammer felt is the ability to provide much brighter sound for strong impact than it does for weak impact forces. It means that the felt stiffness increases also with the rate of loading.

The first work describing an experimental research of a piano hammer *in situ* as an independent object were the remarkable experiments provided by Yanagisawa and Nakamura [1]. In this paper for the first time the main dynamical and very important features of piano hammers were demonstrated: the nonlinearity of the force-compression characteristics of the hammer, the strong dependence of the slope of the loading curve on the hammer velocity, and the significant influence of hysteresis, i.e. the loading and unloading of the hammer felt are not alike. It was shown also that the hammer felt is still deformed even after the acting force is removed.

The most popular model of the hammer in the early eighties was the nonlinear model made by Ghosh [2], who considered the felt as a material obeying the power law

$$F = K u^p, \quad (1)$$

where  $F$  is the acting force,  $u$  is felt compression, and the units for constant  $K$  being  $\text{N/mm}^p$ . But this model cannot describe the hysteretic behavior of the hammer. Further the experimental static testing of different hammers by Hall and Askenfelt [3] demonstrate that for hammers taken from pianos the values of  $p$  ranging from 2.2 to 3.5 give a good approximation of dependence (1). According to Hertz's Law the force acting on two connected locally Hookean bodies gives  $p = 1.5$ . The values of  $p$  different from 1.5 indicate the non-Hooke or the nonlocal felt properties.

A new model that is based on an assumption that the hammer felt made of wool is a microstructural hereditary material was developed and described in [4] in the form

$$F(u(t)) = F_0 \left[ u^p(t) - \frac{\varepsilon}{\tau} \int_0^t u^p(\xi) \exp\left(-\frac{\xi-t}{\tau}\right) d\xi \right]. \quad (2)$$

This is the governing equation connecting the force  $F(u)$  exerted by hammer and the felt compression  $u$ . Here the instantaneous hammer stiffness  $F_0$  and compliance nonlinearity exponent  $p$  are the elastic parameters of the felt, and  $\varepsilon$  and  $\tau$  are the hereditary parameters. According to this hysteretic model, a real piano hammer possesses history-dependent properties, or in other words, its felt made of wool is a material with memory.

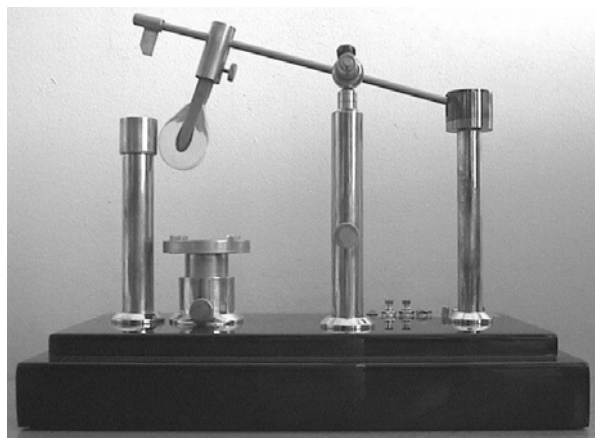


Fig. 1. Piano hammer testing device.

For experimental study of the dynamical felt features a particular piano hammer testing device was built. The device appearance is shown in Fig. 1, and its functioning is described in [5]. This device permits to measure the compression-time and force-time dependencies, and investigate the force-compression characteristics of the hammer felt for the various striking velocities.

Iterated numerical simulations of the dynamical tests obtained the initially unknown values of the hammer parameters. This procedure, which was presented in [5], is based on a mathematical model of the experiments and using the hysteretic model of the felt. In short, the

impact of the hammer can be described by the equation of motion and initial conditions

$$m \frac{d^2 u}{dt^2} + F(u) = 0, \quad u(0) = 0, \quad \frac{du}{dt}(0) = V, \quad (3)$$

Here  $m$  and  $V$  are the hammer mass and the striking velocity, and  $F(u)$  is defined by Eq. (2).

In Fig. 2 are displayed the experimental results of the felt examining for three hammer velocities.

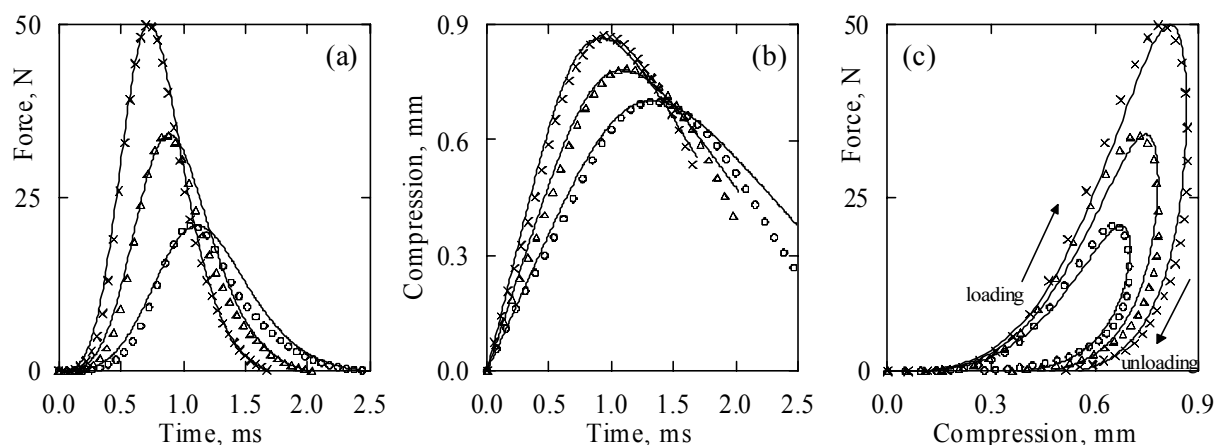


Fig. 2. Comparison of measured data and numerical simulations in a test of a Renner hammer ( $N = 14$ ) showing (a) force histories, (b) compression histories, and (c) force-compression characteristics. The symbols denote measured data for hammer velocities 1.31 m/s (crosses), 1.00 m/s (triangles), and 0.74 m/s (circles). The solid lines are the numerically simulated curves.

The arrows in Fig. 2 (c) show the directions of the compression and decompression branches. The solid lines represent the numerical simulation of the experiment in according to Eq. (3). The experimental results presented in Fig. 2 are quite typical for all the hammers measured. The relationships of dynamic force versus felt compression show the significant influence of hysteresis, so the loading and unloading of the felt are not alike, and the slope of the force-compression characteristics increases with the increasing of the hammer velocity, just like the model of the hysteretic hammer predicts.

All simulated curves in Fig. 2 were obtained by using one and the same combination of hammer parameters:  $F_0 = 8800 \text{ N/mm}^p$ ;  $p = 3.95$ ;  $\varepsilon = 0.992$ ;  $\tau = 2.0 \mu\text{s}$ . Only the value of the hammer striking velocity was varied. The successful matching demonstrated in Fig. 2 is an important result.

Three sets of data, corresponding to three different striking velocities, are matched accurately by simulations using the *same* set of hammer parameters. This result indicates that the hysteretic hammer model gives a good description of real piano hammers.

The presented analytical four-parameter model really describes the dynamic behavior of such a microstructural material as hammer felt. It is also evident that in according to this model some certain set of the felt parameters and a definite rate of loading appoints to one and only unique force-compression curve. It seems that each force-compression curve results in a unique combination of felt parameters and vice versa. However, in spite of this almost evident supposition, the numerical simulation of the felt impact demonstrates that very similar (by eye) force-compression curves can be obtained using the different sets of felt parameters. For example, it was found that the experimental results presented in Fig. 2 can be simulated also by using another felt parameters:  $F_0 = 3520 \text{ N/mm}^p$ ;  $p = 3.95$ ;  $\varepsilon = 0.98$ ;  $\tau = 5.0 \text{ } \mu\text{s}$ . A close and subtle analysis of this phenomenon results in a new and quite another hysteretic model of the felt.

Eliminating the integral term, Eq. (3) with the function (2) may be written also in the form

$$m \frac{d^2 u}{dt^2} + m \tau \frac{d^3 u}{dt^3} + F_0 \left[ (1 - \varepsilon) u^p + \tau \frac{d(u^p)}{dt} \right] = 0 . \quad (4)$$

The analysis of this equation shows that the second term is much smaller than the first one, and also the other terms for any reasonable value of the felt rate loading - up to 10 m/s. Therefore, the second term may be ignored, and introducing new parameters

$$Q_0 = F_0 (1 - \varepsilon), \quad \alpha = \tau / (1 - \varepsilon) , \quad (5)$$

we have

$$m \frac{d^2 u}{dt^2} + Q_0 \left[ u^p + \alpha \frac{d(u^p)}{dt} \right] = 0 . \quad (6)$$

Thus, according to Eq. (3) we can determine the new model of the felt in the form

$$Q(u(t)) = Q_0 \left[ u^p + \alpha \frac{d(u^p)}{dt} \right] = 0 , \quad (7)$$

where  $Q(u)$  is the force exerted by the hammer,  $Q_0$  is the static hammer stiffness, and  $\alpha$  is the time parameter. Such hysteretic three-parameter model is very similar to nonlinear Voigt model and permits a description of the felt compression that is consistent also with experiments.

Both of the models describe the dynamical felt behavior in a similar way. For example, the simulation of the experimental data shown in Fig. 2 may be provided for the same hammer velocities by using the felt parameters:  $Q_0 = 70.4 \text{ N/mm}^p$ ;  $p = 3.95$ ;  $\alpha = 250 \text{ } \mu\text{s}$ . It is more important that these simulated curves are not only exactly alike (by eye) as presented above by solid lines in Fig. 2, but they are also specified by this set of felt parameters uniquely indeed, and it is evident that the both sets of these parameters are related through dependences (5).

The comparison of two models shows that for very slow deformation, the loading and unloading of the hammer felt occur near the limit curve that is the same curve for both hysteretic models determined by

$$F(u) = F_0 (1 - \varepsilon) u^p = Q(u) = Q_0 u^p . \quad (8)$$

However, for very fast loading these two models are quite different. The limit curve for the first four-parameter model is described by equation

$$F(u) = F_0 u^p . \quad (9)$$

With the increasing of loading rate the position of this curve is not changed, but only the amplitude is increased. Instead of this, for the fast loading the limit curve in a frame of the second model does not exist at all, because the force

$$Q(u) = \alpha p V Q_0 u^{p-1} , \quad (10)$$

exerted by hammer in this case is proportional to the striking velocity  $V$ , but this value is unlimited.

Testing of a whole hammer set gives the possibility to describe the continuous variation in the hammer parameters over the compass of the piano. The continuous variations of the hammer parameters versus hammer number  $N$  were obtained by numerical simulation of the experimental data. A best match to the whole set of hammers could be approximated by  $p = 3.7 + 0.015N$ ;  $\varepsilon = 0.9894 + 0.000088N$ ;  $\tau[\mu\text{s}] = 2.72 - 0.02N + 0.00009N^2$ ;  $F_0[\text{kN/mm}^2] = 15.5 \exp(0.059N)$ , for hammer numbers  $1 \leq N \leq 88$ .

The combination of both data concerning the hammer parameters and hammer models can be used as a tool for systematical exploring of the process of the hammer-string interaction. The mathematical modeling of this problem allows predicting the spectrum of the piano string motion, which is very important for piano design. The result of simulation using the traveling-wave model [6] of the string is presented in Fig. 3.

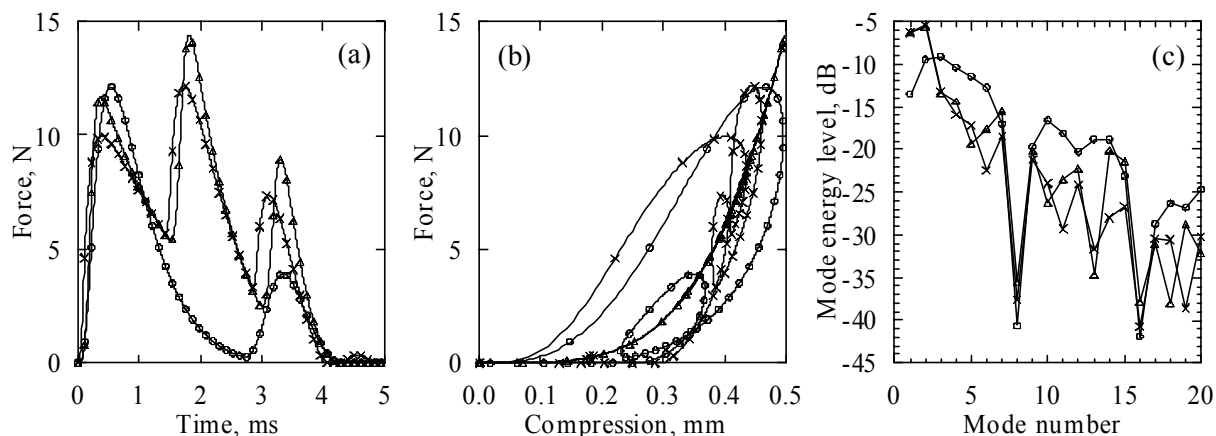


**Fig. 3.** Comparison of string excitation by different hammers showing (a) force histories, (b) force-compression characteristics, and (c) spectra envelopes. The symbols mark the calculated curves in cases of hammer  $N = 21$  (crosses),  $N = 10$  (circles), and non-hysteretic ( $\varepsilon = 0$ ) hammer  $N = 21$  (triangles).

The course of the curves in Fig. 3 (a) clearly demonstrates the arrival of reflected waves. The data in the form of the force-compression characteristics of the hammer felt are useful in the case when hammer strikes the immovable object. If the hammer interacts with vibrating string, due to the complexity of this process we will obtain a very knotty picture shown in Fig. 3 (b). These are the samples of a very nice, but absolutely useless presentation of the obtained results. The spectra of the string motion shown in Fig. 3 (c) were calculated directly from the force histories shown in Fig. 3 (a) using the procedure described in [6].

## REFERENCES

1. Yanagisawa, T., Nakamura, K. Dynamic compression characteristics of piano hammers. // Transactions of Musical Acoustics Technical Group Meeting of the Acoustic Society of Japan. 1982. V.1. P.14-18.
2. Ghosh, M. An experimental study of the duration of contact of an elastic hammer striking a damped piano-forte string. // Indian J. Phys. 1932. V.7. P.365-382.
3. Hall, D. E., Askenfelt, A. Piano string excitation. V. Spectra for real hammers and strings. // J. Acoust. Soc. Am. 1988. V.83. P.1627-1638.
4. Stulov, A. Hysteretic model of the grand piano hammer felt. // J. Acoust. Soc. Amer. 1995. V.97. P.2577-2585.
5. Stulov, A., Mägi, A. Piano hammer testing device. // Proc. Estonian Acad. Sci. Engin. 2000. V.6. P.259-267.
6. Stulov, A. Comparison of string vibration spectra excited by a different piano hammers. // Proc. Institute of Acoustics, ISMA'97. 1997. V.19. Part 5. Book 1. P.231-238.